Effects of Broadband, Bandstop, and Amplitude-Modulated Alternating Current Stimulation on a Neural Mass Model*

Alexander Pei[1] and Barbara G. Shinn-Cunningham[1,2]

2022 IEEE Biomedical Circuits and Systems Conference (BioCAS) | 978-1-6654-6917-3/22/$31.00 ©2022 IEEE | DOI: 10.1109/BioCAS54905.2022.9948583

***Abstract*— tACS is a neuromodulatory technique used to investigate the role of neural oscillations by modulating endogenous electrical fields. Typically, the brain is stimulated at one of its eigenfrequencies, associated with a particular cognitive process. However, novel stimulation protocols have been hypothesized to better entrain neural oscillators by stimulating with a broader range of frequencies near the eigenfrequency. Also, stimulation waveforms bandstopped around eigenfrequency are thought to desynchronize the neural network. Amplitude-modulated tACS has also been proposed to evade the stimulation artifact introduced during EEG-tACS recordings. We explored the effects of these various stimulation parameters using a Jansen and Ritt neural mass model. We found no significant differences between broadband and single peak stimulation, but did find that bandstop filtered stimulation was able to desynchronize the neural network. We also found that amplitude-modulated tACS was not able to entrain the network at the low-frequency component of the AM signal.**

I. INTRODUCTION

During cognitive processing, the brain exhibits rich oscillatory dynamics as a result of synchronized firing among neural populations. While originally speculated to be epiphenomenon of neural computation, neuromodulatory techniques have established a functional role of brain oscillations. Transcranial alternating current stimulation (tACS) is one neuromodulatory technique that applies an external sinusoidal electrical current through the scalp to alter electric fields within the cortical tissue [1]. By first observing the frequency and location of oscillations during a cognitive task, one can match the frequency and location of said oscillations with tACS. This may produce more robust effects when trying to bias cognitive behavior. For example, $8-14$ Hz alpha waves appear in the parietal cortex ipsilateral to the attended hemifield of acoustical [2] and visual [3] space. Applying alpha wave tACS to the parietal cortex has been shown to bias attention towards the side ipsilateral to the site of stimulation [4]–[6].

Despite several accounts of tACS establishing a functional role of neural oscillations in cognitive processing, there exists both experimental limitations and an incomplete understanding of the technology as a whole. This is due to the enormous electrical artifact tACS introduces into EEG recordings; the electrical artifact obscures how tACS affects endogenous oscillations [7]. One of the mechanisms through which tACS can operate is the Arnold tongue perspective of dynamical systems, which says that a dynamical system is more strongly entrained by an oscillation closer to its eigenfrequency [8]. This is supported through computational models of neural systems under the influence tACS, which show this effect [9]. In humans, the peak alpha frequency during attention can vary across subjects [10], and the modulation of behavior during cognitive tasks depends on whether subjects are stimulated at individualized alpha frequencies [11].

Novel tACS experiments aim to expand on these findings by creating new stimulation protocols. One such modification attempts to expand on the notion of individualized stimulation frequencies to better modulate neural dynamics [12]. Instead of delivering current at a single peak frequency, broadband current stimulation delivers current with a broader power distribution ($\pm 1-2$ Hz peak frequency). This is motivated by neural oscillatory dynamics that show a broad range of peak frequencies during a particular cognitive task. Additionally, the broad peak of frequencies can represent different neural processes superimposed upon one another [13]. Thus, stimulating over a broader range of frequencies could drive a larger range of neural circuits. This has also lead to the idea of stimulating the brain with oscillations bandstopped around the peak frequency in an attempt to desynchronize oscillations at the peak frequency. However, the only human experiment investigating these stimulation protocols found that broadband, single peak, and bandstopped oscillations all had similar perceptual effects to one another [12].

Another stimulation protocol attempted to bypass the presence of the tACS stimulation artifact by using amplitude-modulated (AM) tACS, where a high-frequency carrier waveform is modulated by a low-frequency envelope waveform [14]. The carrier waveform is designed to have a frequency much higher (>100 Hz) than endogenous neural oscillations in order to ensure that it does not have any effects on the neural dynamics. The low-frequency envelope is designed to modulate the frequency of interest in the brain. Because the spectral content of the AM waveform is concentrated around the carrier frequency, low-pass filtering the EEG data below the carrier frequency would effectively remove the entire tACS artifact. Human studies found conflicting results, where phosphene induction only depended on the carrier frequency rather than the envelope frequency [14].

To shed light on these mechanisms, we employed a

*This work was supported by grant from the N00014-18-1-2069 Office of Naval Research.

[1]Alexander Pei (email: apei2@andrew.cmu.edu) and Barbara G. Shinn-Cunningham (email: bgsc@andrew.cmu.edu) are with the Department of Electrical and Computer Engineering, Carnegie Mellon University, Pittsburgh, PA 15213, USA

[2]Barbara Shinn-Cunningham is also with the Neuroscience Institute, Carnegie Mellon University, Pittsburgh, PA 15213, USA

Jansen and Ritt neural mass model (NMM) to investigate the impact of broadband, bandstopped, and AM-tACS on simulated neural dynamics. We found no significant differences between broadband and single peak tACS. However, we found that bandstopped tACS suppressed peak power in the bandstopped range. We also found that AM-tACS did not entrain the model near the modulation frequency, unless the amplitude signal was greatly increased.

II. Methods

A. Jansen and Ritt neural mass model

To model coritcal dynamics, we used a Jansen and Ritt neural mass model (NMM) consisting of interconnected layers of excitory interneurons, pyramidal cells, and inhibitory interneurons. The membrane potential of each subpopulation is modeled as a dampened spring with nonlinear displacement, where the displacement of one subpopulation is the sum of all the firing rates entering into said subpopulation. The nonlinearity is introduced via a sigmoid function, which maps membrane potentials into firing rates. The subpopulations are connected such that the excitatory and inhibitory interneurons depolarize and hyperpolarize the pyramidal cells respectively, while the pyramidal cells depolarize both the excitatory and inhibitory interneurons. We applied current stimulation only to the pyramidal cell layer because their orthogonality with respect to the scalp results in the strongest effects from the applied electric field. A diagram and table of the model and model parameters can be seen in Fig. 1 and Tab. I.

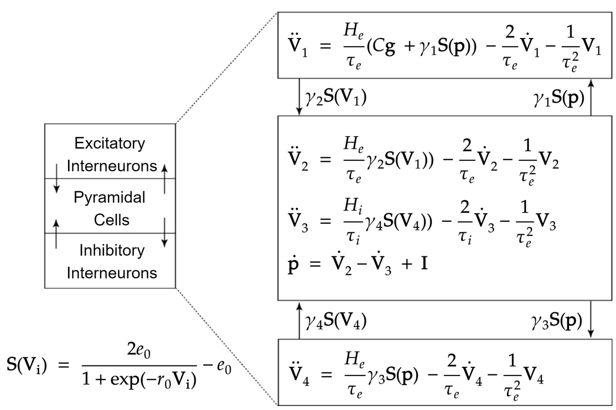

Fig. 1. A schematic of the NMM. V_1 and V_4 are the membrane potentials of the excitatory and inhibitory interneurons. V_2 and V_3 are the depolarizing and hyperpolarizing currents of the pyramidal cells. p is the net pyramidal cell membrane depolarization. I is the injected current. $S(\cdot)$ is the sigmoid function which converts membrane potentials into firing rates. g is the normally distributed random noise input signal with a mean of 0 and a standard deviation of 0.05.

B. Broadband and bandstop stimulation

The dynamics of the NMM were first simulated without current stimulation, and the peak power of the model was found to centered at 4 Hz. The pyramidal cell response was both bandpassed and bandstoppped between $3-5$ Hz using a fourth-order Butterworth filter. The power of both signals was normalized such that the sum of the squared magnitude of the FFT coefficients of the signals both equaled the power of a pure sine wave at 4 Hz with an amplitude of 2. This was done to remove the potential confounds of total signal power affecting neural dynamics [12].

TABLE I
Model hyperparameters

Parameter	Description	Value
H_e, H_i	Max amplitude of post-synaptic potential	3.25, 29.3 (mV)
τ_e, τ_i	Lumped time constants of dendritic delays	10, 15 (s^{-1})
e_0	Max firing rate of neural population	2.5 (s^{-1})
r_0	Steepness of the sigmoid function	0.56 (mV^{-1})
$\gamma_1 \ldots \gamma_4$	Number of synapses in neural population	50, 40, 12, 12
C	Connectivity scalar for extrinsic inputs	1000

C. Amplitude modulated stimulation

The AM current stimulation was calculated as follows:

$$I(t) = \sin(2\pi f_c t) + \sin(2\pi(f_c + f_m)t) \qquad (1)$$

where f_c and f_m are the carrier and modulation frequency. This produced an AM signal with a peak of 2. We investigated different carrier frequencies (100, 200, 500 Hz) as well as fixing the carrier frequency at 100 Hz and increasing the amplitude of the signal (8, 16, and 32).

D. Simulation

The state equations in Fig. 1 were implemented in Matlab Simulink. The simulation was run with a timestep of 0.001 seconds. For each simulation, the model parameters were each scaled between $[0.5, 1.25]$, drawn from a uniform distribution to introduce variability between runs. 100 sets of parameters were generated in this way (to simulate 100 different subjects). For each set of parameters (which we refer to as subjects for the rest of the paper), the simulation was repeated 10 times with different random noise seeds. Across all various stimulation waveform conditions, the random noise seeds were kept consistent. For a given trial n and a particular subject, the pyramidal cell signal used to generate the bandpass and bandstop signals was *not* from trial n, to ensure that information about the random noise would not carry over and confound the effects of the stimulation.

III. Results

A. Single peak, broadband, and bandstop stimulation

A single trial along with examples of the various stimulation waveforms and power spectra can be seen in Fig. 2. The membrane depolarization of the pyramidal cell layer has a broadband spectrum ranging from $0-20$ Hz, with a peak at around 4 Hz.

Fig. 3 shows the average power spectra for the various stimulation conditions, where broadband and single peak stimulation resulted in the model having higher 4 Hz power, while bandstop stimulation reduced 4 Hz power. Fig. 4 shows 4 Hz power for individual subjects. A repeated-measures ANOVA found a significant effect on the type of stimulation waveform and 4 Hz power ($F(3,99) = 2424, p < 0.001$). Paired-sample T-tests also supported this finding; 4 Hz power

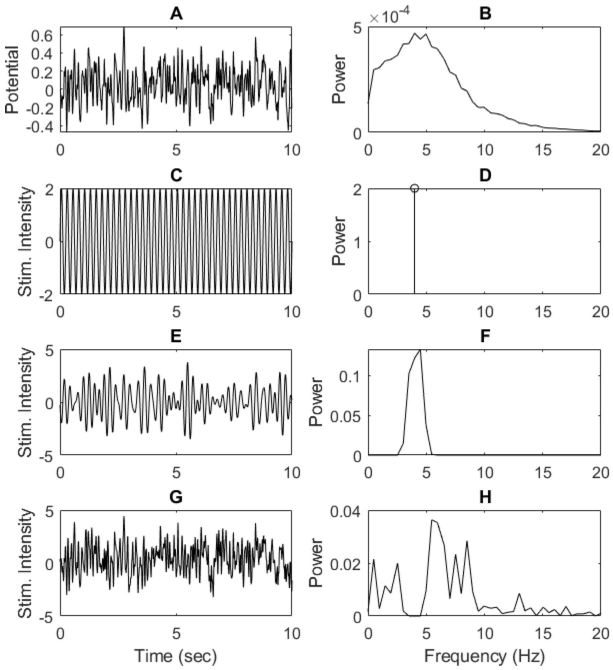

Fig. 2. The time series (A) and power spectrum (B) of the pyramidal cell depolarization for a single trial with arbitrary units. (C) 4 Hz stimulation waveform and (D) power spectrum. (E) Bandpass waveform of the waveform in (A) at $3-5$ Hz and with normalized power spectrum (F). (G) Bandstop waveform of the waveform in (A) at $3-5$ Hz and with normalized power spectrum (H).

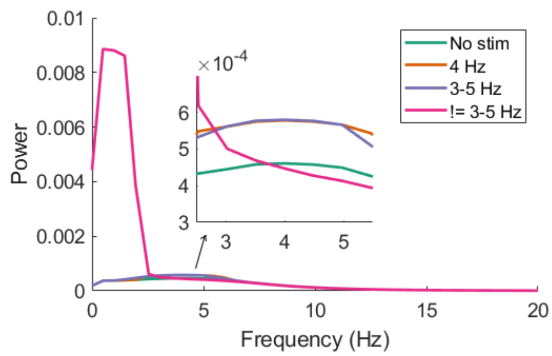

Fig. 3. Power spectrum with arbitrary units for the four different stimulation parameters, with an additional zoomed-in view around 4 Hz. No stim is no stimulation, 4 Hz is single peak stimulation, $3-5$ Hz is broadband stimulation, $!=3-5$ Hz is bandstop stimulation.

was higher in the 4 Hz stimulation vs. No stimulation condition $(t(99) = -76.95, p < 0.001)$. Broadband $3-5$ Hz was also greater than No stimulation $(t(99) = -76.64, p < 0.001)$. No stimulation had higher 4 Hz power than bandstop stimulation $(t(99) = -7.23, p < 0.001)$. Broadband stimulation did not significantly increase 4 Hz power compared to 4 Hz stimulation $(t(99) = -0.683, p = 0.248)$.

B. AM-tACS

A sample AM-tACS waveform and spectrum can be seen in Fig. 5. The effects of various carrier frequencies (100 Hz, 200 Hz, 500 Hz) with a modulation frequency of 4 Hz and an amplitude of 2 is shown in Fig. 6. A repeated-measures

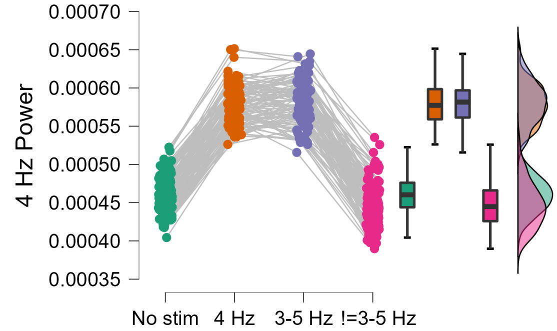

Fig. 4. 4 Hz power for the four different stimulation parameters. Each dot represents a set of randomized parameters (a different "subject") with the power spectrum averaged over the 10 trials.

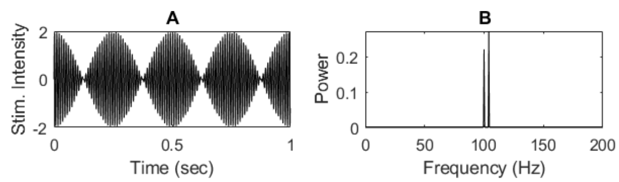

Fig. 5. A sample AM-tACS (A) waveform and power spectrum (B) with a carrier frequency f_c = 100 Hz and a modulation frequency of f_m = 4 Hz.

ANOVA test found a significant difference between peak 4 Hz power and carrier frequency $(F(3,99) = 3.3363, p = 0.018)$; however, these differences are minuscule. Paired t-tests comparing peak 4 Hz power found no difference between 100 Hz carrier vs. No stimulation $(t(99) = 1.007, p = 0.842)$ and no difference between 200 Hz carrier vs. No stimulation $(t(99) = 1.007, p = 0.945)$. 500 Hz carrier was greater than No stimulation $(t(99) = -2.328, p = 0.011)$.

We also explored changing the amplitude of the AM signal with a fixed carrier frequency of 100 Hz while varying the amplitude of the AM signal from 2 to 4, 8, 16, and 32 to see if increasing the stimulation intensity would be able to drive the NMM at 4 Hz. The results for the 100 subjects can be seen in Fig. 7. Paired t-tests found that 4 Hz power was increased with respect to No stimulation for the various amplitudes: 8 $(t(99) = -1.773, p = 0.004)$, 16 $(t(99) = -5.642, p < 0.001)$, and 32 $(t(99) = -13.39, p < 0.001)$.

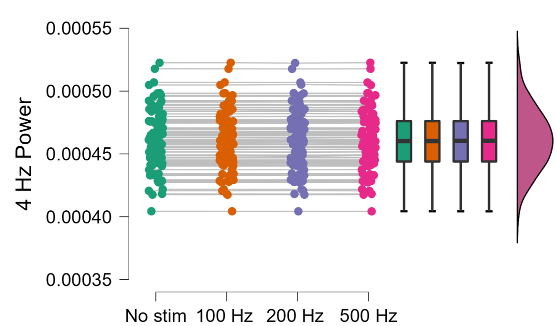

Fig. 6. 4 Hz power for the three different carrier frequencies as well as no stimulation. Each dot represents a set of randomized parameters with the power spectrum averaged over the 10 trials.

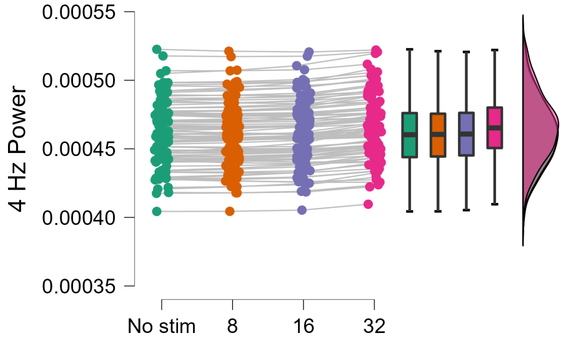

Fig. 7. 4 Hz power for the varying amplitudes for the AM-tACS. Each dot represents a set of randomized parameters with the power spectrum averaged over the 10 trials.

IV. Discussion

tACS is a neuromodulatory technique that can establish a functional role of neural oscillations in the brain. Novel experimental designs use stimulation protocols that not only target the peak frequency of a neural oscillator, but also a broadband of peak frequencies in an attempt to entrain a neural network more effectively. A spectral inverse of the broadband stimulation acquired by bandstop filtering around the peak frequency has also been hypothesized to suppress activity at the eigenfrequency of a neural network. Additionally, amplitude-modulated tACS has been proposed as a method to evade the electrical artifact introduced during simultaneous tACS and EEG. In this work, we explored these various stimulation parameters by modeling neural activity and the effects of tACS via a NMM.

In our first experiment, we explored the effects of single peak, broadband, and bandstop stimulation waveforms. We expected broadband stimulation to better entrain the neural network, given that the peak frequency of the NMM was broadband in nature and not narrowbanded. However, we found no significant difference between single peak stimulation and broadband stimulation. Because the stimulation waveforms were normalized to have equal power, this might suggest that the cross-frequency interactions of the power transfer function in the range of $3-5$ Hz are similar. Stimulating the NMM with bandstop stimulation was able to suppress the activity at the peak frequency of 4 Hz, suggesting negative cross-frequency interactions within and outside of the peak frequency. This also suggests that it would be possible to do offline analysis of EEG dynamics to determine cross-frequency interactions, followed by tACS to target those cross-frequency interactions.

The second experiment investigated whether AM-tACS could modulate the NMM at peak 4 Hz frequency, despite the power spectrum having power concentrated at a high-frequency carrier. We found that AM-tACS was unable to entrain the network at its eigenfrequency compared to a pure sinusoidal input with equal amplitude, regardless of the carrier frequency. Only when the amplitude was increased to a drastically higher value was the network able have a miniscule effect on the eigenfrequency. This is in agreement with another AM-tACS computational model [15]. This may suggest that AM-tACS may not be an effective way to drive neural dynamics at the modulation envelope, encouraging the development of alternative stimulation parameters and artifact removal algorithms to analyze EEG recorded during tACS.

References

[1] A. Liu, M. Vöröslakos, G. Kronberg, S. Henin, M. R. Krause, Y. Huang, A. Opitz, A. Mehta, C. C. Pack, B. Krekelberg, A. Berényi, L. C. Parra, L. Melloni, O. Devinsky, and G. Buzsáki, "Immediate neurophysiological effects of transcranial electrical stimulation," *Nature Communications 2018 9:1*, vol. 9, pp. 1–12, 11 2018.

[2] L. M. Bonacci, L. Dai, and B. G. Shinn-Cunningham, "Weak neural signatures of spatial selective auditory attention in hearing-impaired listeners," *The Journal of the Acoustical Society of America*, vol. 146, p. 2577, 10 2019.

[3] T. A. Rihs, C. M. Michel, and G. Thut, "Mechanisms of selective inhibition in visual spatial attention are indexed by -band eeg synchronization," *European Journal of Neuroscience*, vol. 25, pp. 603–610, 1.

[4] T. Schuhmann, S. K. Kemmerer, F. Duecker, T. A. de Graaf, S. ten Oever, P. de Weerd, and A. T. Sack, "Left parietal tacs at alpha frequency induces a shift of visuospatial attention," *PLOS ONE*, vol. 14, p. e0217729, 11.

[5] Y. Deng, R. M. Reinhart, I. Choi, and B. Shinn-Cunningham, "Causal links between parietal alpha activity and spatial auditory attention," *eLife*, vol. 8, 11 2019.

[6] M. Wöstmann, J. Vosskuhl, J. Obleser, and C. S. Herrmann, "Opposite effects of lateralised transcranial alpha versus gamma stimulation on auditory spatial attention," *Brain Stimulation*, vol. 11, pp. 752–758, 7 2018.

[7] S. Kohli and A. J. Casson, "Removal of gross artifacts of transcranial alternating current stimulation in simultaneous eeg monitoring," *Sensors (Switzerland)*, vol. 19, 2019.

[8] W. A. Huang, I. M. Stitt, E. Negahbani, D. J. Passey, S. Ahn, M. Davey, M. Dannhauer, T. T. Doan, A. C. Hoover, A. V. Peterchev, S. Radtke-Schuller, and F. Fröhlich, "Transcranial alternating current stimulation entrains alpha oscillations by preferential phase synchronization of fast-spiking cortical neurons to stimulation waveform," *Nature Communications 2021 12:1*, vol. 12, pp. 1–20, 5 2021.

[9] M. M. Ali, K. K. Sellers, and F. Fröhlich, "Transcranial alternating current stimulation modulates large-scale cortical network activity by network resonance," *Journal of Neuroscience*, vol. 33, pp. 11 262–11 275, 7 2013.

[10] A. W. Corcoran, P. M. Alday, M. Schlesewsky, and I. Bornkessel-Schlesewsky, "Toward a reliable, automated method of individual alpha frequency (iaf) quantification," *Psychophysiology*, vol. 55, p. e13064, 7 2018.

[11] G. Mioni, A. Shelp, C. T. Stanfield-Wiswell, K. A. Gladhill, F. Bader, and M. Wiener, "Modulation of individual alpha frequency with tacs shifts time perception," *Cerebral Cortex Communications*, vol. 1, pp. 1–9, 8 2020.

[12] S. E. Janssens, S. T. Oever, A. T. Sack, and T. A. de Graaf, ""broadband alpha transcranial alternating current stimulation": Exploring a new biologically calibrated brain stimulation protocol," *NeuroImage*, vol. 253, p. 119109, 6 2022.

[13] C. S. Benwell, R. E. London, C. F. Tagliabue, D. Veniero, J. Gross, C. Keitel, and G. Thut, "Frequency and power of human alpha oscillations drift systematically with time-on-task," *NeuroImage*, vol. 192, pp. 101–114, 5 2019.

[14] C. Thiele, T. Zaehle, A. Haghikia, and P. Ruhnau, "Amplitude modulated transcranial alternating current stimulation (am-tacs) efficacy evaluation via phosphene induction," *Scientific Reports 2021 11:1*, vol. 11, pp. 1–10, 11 2021.

[15] E. Negahbani, F. H. Kasten, C. S. Herrmann, and F. Fröhlich, "Targeting alpha-band oscillations in a cortical model with amplitude-modulated high-frequency transcranial electric stimulation," *NeuroImage*, vol. 173, pp. 3–12, 6 2018.